VELOCITY FIELD OF A ROUND TURBULENT TRANSVERSE JET

Suman Muppidi
University of Minnesota,
Minneapolis, Minnesota 55455, USA
suman@aem.umn.edu

Krishnan Mahesh
University of Minnesota,
Minneapolis, Minnesota 55455, USA
mahesh@aem.umn.edu

ABSTRACT

Direct numerical simulations are used to study a round turbulent jet in a laminar crossflow. The velocity ratio is 5.7 and the Reynolds number is 5000. Mean velocity and turbulent intensity profiles available from experiment (Su & Mungal 2004) are compared to simulation results, and good agreement is observed. A two-dimensional model problem is used to study the evolution of the jet cross-section and the counter-rotating vortex pair (CVP). The model problem shows how the trailing edge of the jet deforms and yields a CVP at later times. The initial stages of the evolution are at constant acceleration; i.e. pressure-driven while the later stages are at constant velocity; i.e. momentum driven. The model problem is used to suggest a pressure-based argument for CVP formation.

INTRODUCTION

Jets in crossflow, also called 'transverse jets' are defined as the flow field where a jet of fluid enters and interacts with a crossflowing fluid. Examples of jets in crossflow are fuel injectors, smokestacks and dilution holes in gas turbine combustors. Past work on this problem includes the study of the velocity and vorticity fields (Kamotani & Greber 1972, Fearn & Weston 1974, Andreopoulos & Rodi 1985, Fric & Roshko 1994, Krothapalli *et al.* 1990, Kelso & Smits 1995), study of the scalar field and mixing (Smith & Mungal 1998, Shan & Dimotakis 2000, Su & Mungal 2004) and attempts at modeling the flow field and jet trajectory (Broadwell & Breidenthal 1984, Karagozian 1986, Hasselbrink & Mungal 2001a, Muppidi & Mahesh 2005a).

Broadwell & Breidenthal(1984) conclude that the global length scale in the flow is rd in the region away from the jet exit. This length scale is used to scale the trajectory as

$$\frac{y}{rd} = A\left(\frac{x}{rd}\right)^B \tag{1}$$

where A and B are constants. Pratte & Baines (1967) obtain A=2.05 and B=0.28 using their experimental data. Margason (1993) provides a list of experimental values for A and B. Experimental results show $1.2 < A < 2.6$ and $0.28 < B < 0.34$. Smith & Mungal (1998) use their experimental results ($5 < r < 25$) and observe that the trajectories scale best with rd (as compared to scaling with d or r^2d). Experimentally obtained trajectories, of jets at different velocity ratios, show a significant scatter when normalized using rd. Muppidi & Mahesh (2005a) show, using controlled numerical simulations, that the jet trajectory is sensitive to the velocity profiles of the jet and of the crossflow. Since the rd scaling does not contain any information on these profiles, the rd–scaled trajectories show a significant scatter. A model is proposed, that explains the jet trajectory in terms of the inertias of the jet and of the crossflow. An analytical expression is derived for the near–field parameter h, which is defined as the height up to which the jet is vertical before bending into the crossflow. It is shown that the scatter reduces considerably when the trajectories are scaled using h.

Some of the recent work on jets in crossflow involves numerical simulations. Although RANS calculations (Chochua *et al.* 2000) predict the mean velocities reasonably, turbulent intensity predictions can vary significantly from experimental results. Acharya *et al.* (2001) provide a summary of the different numerical attempts to model jets in crossflow. They conclude that DNS and LES were better able to predict the mean velocities and turbulence intensities (as compared to the two–equations model and RSTM predictions). Yuan *et al.* (1999) performed LES of a round jet in crossflow and showed reasonable agreement for mean velocities and turbulent intensities with experimental results of Sherif & Pletcher (1989). Schluter & Schonfeld (2000) compared the results of their LES with experimental velocity profiles of Andreopoulos & Rodi (1984) and scalar fields of Smith & Mungal (1998), and obtain reasonable agreement with the experiments.

This paper is organized in two parts. In part I, results of DNS of a turbulent jet in crossflow are presented. Part II discusses a two–dimensional model problem used to study the evolution of the jet cross–section.

SIMULATION DETAILS

Problem

Simulations are performed under the same conditions as experiments by Su & Mungal (2004). The velocity ratio is 5.7 and the Reynolds number of the flow, based on the bulk jet velocity and the jet–exit diameter is 5000. In the experiment, the jet exits out of a round pipe (about 70 d in length) into the crossflow. In the absence of any crossflow, fully developed pipe flow conditions are expected at the jet–exit (Su & Mungal,

section 2). The crossflow is laminar and the 80% boundary layer thickness is $\delta_{80\%} = 1.32d$ at the location of the center of the jet–exit, and in the absence of the jet.

Numerical Details

The numerical scheme solves the incompressible Navier Stokes equations on unstructured grids. The scheme has been described by Mahesh *et al.* (2004) and is not dealt with here in detail. The algorithm stores the cartesian velocities and the pressure at the centroids of the cells (control volumes) and the face normal velocities are stored independently at the centroids of the faces. The scheme is a predictor–corrector formulation which emphasizes discrete energy conservation on unstructured grids. This property makes the algorithm robust at high Reynolds numbers without numerical dissipation. Time–stepping is implicit and is performed using a Crank–Nicholson scheme. The algorithm has been validated for a variety of problems (details are provided in Mahesh *et al.* 2004) over a range of Reynolds numbers.

The computational domain used in the simulations spans $36d \times 64d \times 64d$ in the x, y & z directions respectively, and includes a $2d$ length of the pipe. This allows the jet fluid to develop naturally before exiting into the crossflow. The importance of solving for flow in the pipe was noted by Yuan *et al.* (1999) and Muppidi & Mahesh (2005a). The computational mesh is unstructured and consists of hexahedral elements. A total of 11 million control volumes are used to generate the present mesh. The computations are initialized with just the crossflow, and the solution is allowed to develop for about 80 d/u_∞ units before statistics are computed. This way, statistics are computed only after the transients exit the domain. The computational time step is 0.0025 d/u_∞.

RESULTS

Part I. DNS of turbulent jet in crossflow

In order to simulate a turbulent jet in crossflow, a separate simulation of a fully turbulent pipe flow was performed. The velocity field at a cross–section from that simulation was stored over a length of time and interpolated as the boundary condition for the jet in the turbulent jet simulation. The crossflow is laminar, and in the absence of the jet, the velocity field corresponds to the self–similar Blasius boundary layer solution. Figure 1(a) shows contours of instantaneous vorticity magnitude $\sqrt{\omega_x^2 + \omega_y^2 + \omega_z^2}$ on the symmetry plane, along with an instantaneous streamline passing through the center of the jet–exit. The highest vorticity magnitude (shown in blue) is observed near the walls of the pipe and along the jet. Note that the simulation resolves the small scales of motion inside the pipe and close to the jet exit. Small scale features are observed even away from the jet–exit along the jet centerline. Upstream of the jet, crossflow fluid shows a vorticity that is steady, smaller in magnitude, and is characteristic of a laminar boundary layer. Downstream of the jet (and $x/d <$ 6), there appears to be a quiescent region with low vorticity (shown in white). Further downstream, the flow contains larger scale features which move slowly in the direction of the crossflow.

Figure 1(a) also shows that the jet is asymmetric about the center streamline. The jet is wider downstream (positive x

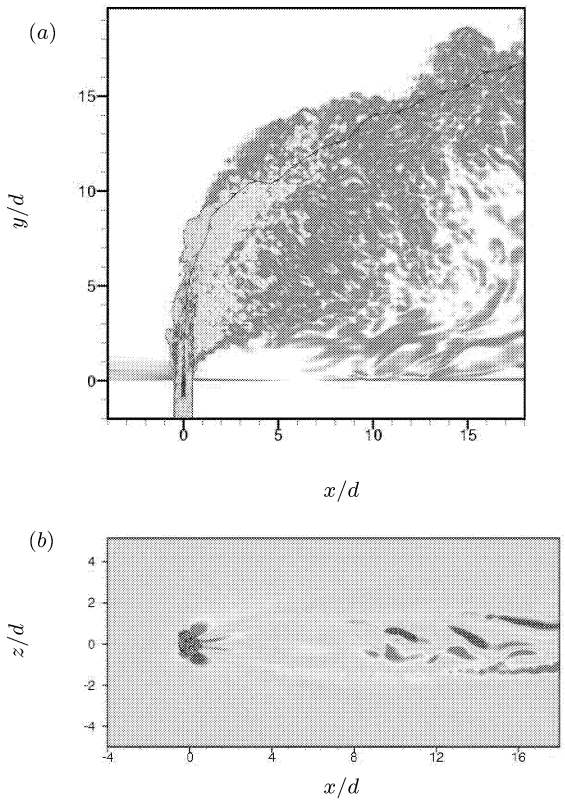

Figure 1: (a) Instantaneous contours of vorticity magnitude $\sqrt{\omega_x^2 + \omega_y^2 + \omega_z^2}$ on the symmetry plane. (b) Instantaneous contours of ω_y on the horizontal plane $y/d = 0.1$.

side of the centerline) as compared to the upstream side. This asymmetry has been noted by Su & Mungal (2004, figure 8) and they suggest it is due to the 'jet fluid that is stripped away from the developing region of the jet by the crossflow and is deposited in the wake region', suggesting that the jet fluid seen downstream of the streamline exits the jet–exit lying on the periphery (of the jet) and not on the symmetry plane. Also note that the crossflow fluid has a higher momentum upstream side of the jet (negative x side of the jet centerline) as compared to the downstream side (the 'wake' region). The asymmetry in the jet width could be accentuated by this difference in momentum.

Instantaneous contours of ω_y on the horizontal plane y/d = 0.1 are shown in figure 1(b). Note the separation of the crossflow boundary layer a few diameters downstream of the jet–exit.

Comparison to experiments.

Su & Mungal (2004) provide detailed experimental profiles of velocity and turbulent intensities at three stations (y/rd = 0.1, 0.5 and 1.0), as a function of the non–dimensionalized streamwise distance (x/rd). The fluid density of the jet and of the crossflow are assumed to be same in the present simulation. The jet in the experiment, however, has a 10% higher density than the crossflow (ρ_j/ρ_∞ = 1.1, Su & Mungal 2004). In order to account for this difference in densities, the profiles

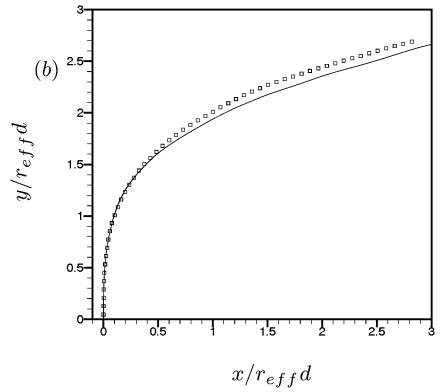

Figure 2: Comparison of jet trajectory from the simulation (———) to that from the experiment (□).

are normalized with r_{eff}, where

$$r_{eff}{}^2 = \frac{\rho_j \overline{u_j}^2}{\rho_\infty {u_\infty}^2} = \frac{\rho_j}{\rho_\infty} r^2. \qquad (2)$$

The value of r_{eff} is 5.7 in the simulation and 6.008 in the experiment. Figure 2 compares the jet trajectories from the simulation and the experiment. Trajectories are scaled using r_{eff} and good agreement is obtained. At a location $15d$ downstream of the jet–exit, the difference between the scaled trajectories is 2.8%.

Profiles of $\overline{v}$, $\overline{v'v'}$, $\overline{u'u'}$ and $\overline{u'v'}$ are compared in figure 3. These profiles correspond to locations $y/r_{eff}d = 0.1$, 0.5 and 1.0 on the symmetry plane. The solid lines in these plots are results from the present simulation while the symbols are results from the experiment. Overall, for all the quantities compared and at all the locations, the agreement presented is quite reasonable, particularly the context of the sharp gradients that the profiles possess (*e.g.* $\overline{v'v'}$ and $\overline{u'v'}$ at $y/r_{eff}d = 0.1$). The comparison is discussed in more detail by Muppidi & Mahesh (2005b).

The mean velocity ($\overline{v}$) profiles show that at the station closest to the jet–exit, the behavior exhibited by the jet is similar to that of a turbulent pipe flow. This is indicated by the apparent symmetry of the profile about the centerline. Moving away from the jet–exit, fluid downstream of the jet demonstrates an increase in velocity and at the farthest station, the profile is indicative of two distinct jets. The jet fluid that is stripped off the jet edges and deposited downstream possesses a vertical velocity and results in the profile as observed in figure 3(a)(at $y/r_{eff}d = 1.0$). Contours of time–averaged magnitude of velocity, when plotted on the symmetry plane, also show this distinctive 'two–jet' behavior.

Part II. Model problem to study jet evolution

A circular jet, issuing into a crossflow bends in the direction of the crossflow. Yuan & Street (1998) explain the bending of the jet as a result of the pressure 'drag' in the near field and in terms of the entrainment in the far–field. Muppidi & Mahesh (2005a) explain the jet trajectory in terms of the competing inertias of the jet and crossflow fluids. As the jet bends, a pair of counter–rotating vortices (CVP) are formed. The CVP is a 'signature' feature of this flow and has been the subject of much investigation. In particular, different mechanisms have

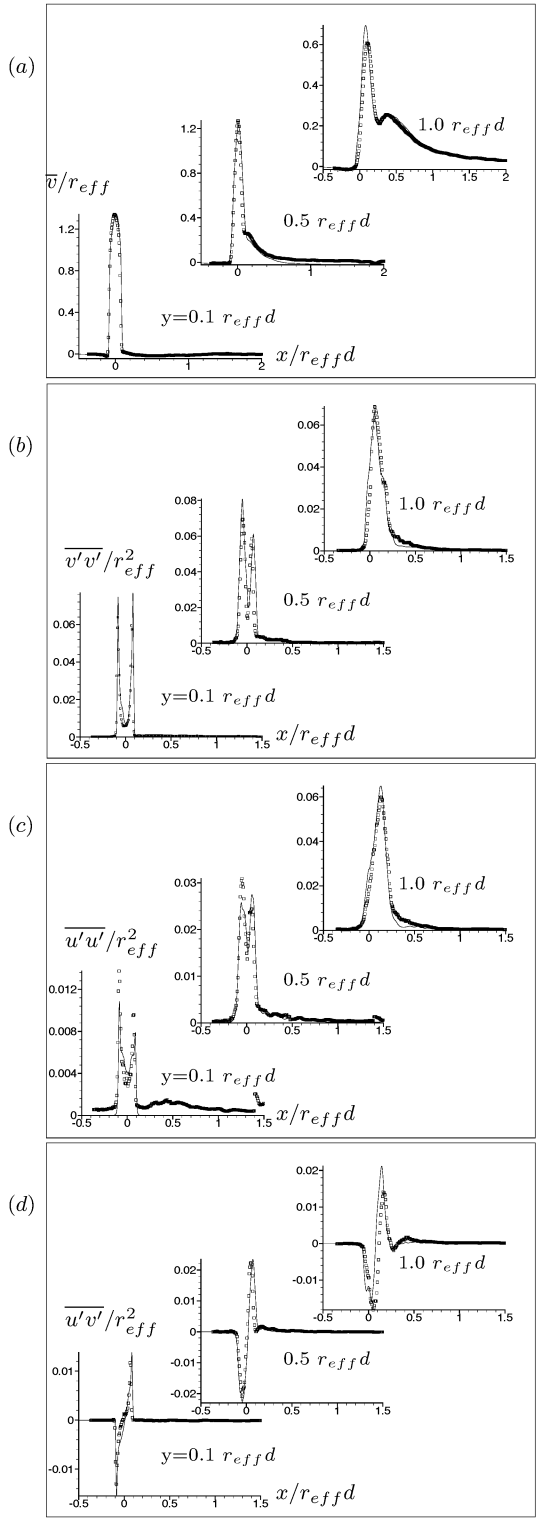

Figure 3: Comparison of mean vertical velocity ($\overline{v}$) and turbulent intensity ($\overline{v'v'}$, $\overline{u'u'}$ and $\overline{u'v'}$) profiles with the experimental results. ——— simulation, □ experiment.

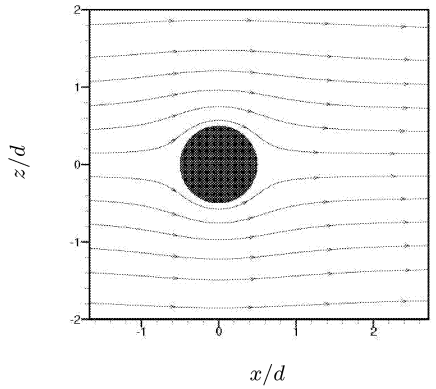

Figure 4: Initial condition of the model problem used to study the evolution of the jet. Streamlines show the potential flow past a circular cylinder, while the contours show out–of–plane velocity.

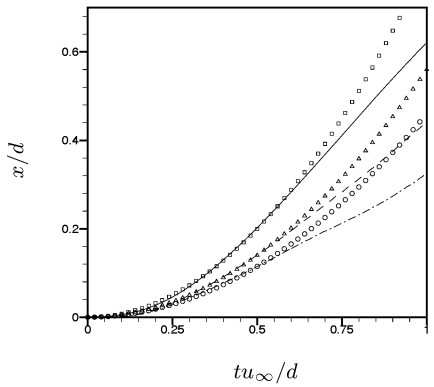

Figure 5: Position of the jet plotted against the temporal variable. ——— : Re = 1000, – – – – : Re = 10000 & —·— : Re = 100000. Symbols show quadratic curve fits to each of the trajectories.

been suggested for formation of the CVP. It has been suggested (Andreopoulos & Rodi 1984 etc.) that the CVP is formed by the shear layer emanating from the pipe. Coelho & Hunt (1989) suggest that the CVP is initiated within the pipe. Kelso *et al.* (1996) conclude from their experiments that CVP roll–up is related to the separation inside the pipe and that the jet shear layer 'folds', contributing to the CVP formation. The cross–section of a jet issuing out of a circular jet–exit is known to deform to an oval, and then to a kidney shape. Smith & Mungal (1998) show that this evolution of the jet is slower at r=20 than at r=10.

A two–dimensional model problem is studied in order to understand the evolution of the jet cross–section. The initial condition of the problem, shown in figure 4, is as follows. A circular region of diameter d is defined. The fluid inside this region has a uniform vertical velocity ($v = v_j$) and zero in–plane velocity ($u,\ w = 0$). The fluid outside this region is prescribed to have an in–plane velocity ($u,\ w$) corresponding to potential flow past a circular cylinder, and a zero vertical velocity ($v = 0$). The fluid inside the circle simulates the jet and the fluid outside of it simulates the crossflow. The direction of the crossflow fluid is from left to right. Uniform crossflow velocity (u_∞) is specified at the crossflow inflow and the spanwise boundary planes. The governing equations for momentum are

$$\frac{\partial u}{\partial t} + u\frac{\partial u}{\partial x} + w\frac{\partial u}{\partial z} = -\frac{\partial p}{\partial x} + \nu\left\{\frac{\partial^2 u}{\partial x^2} + \frac{\partial^2 u}{\partial z^2}\right\},$$

$$\frac{\partial w}{\partial t} + u\frac{\partial w}{\partial x} + w\frac{\partial w}{\partial z} = -\frac{\partial p}{\partial z} + \nu\left\{\frac{\partial^2 w}{\partial x^2} + \frac{\partial^2 w}{\partial z^2}\right\} \quad \text{and}$$

$$\frac{\partial v}{\partial t} + u\frac{\partial v}{\partial x} + w\frac{\partial v}{\partial z} = \nu\left\{\frac{\partial^2 v}{\partial x^2} + \frac{\partial^2 v}{\partial z^2}\right\}. \qquad (3)$$

Note that u and w are not affected by the out–of–plane velocity component v. Also note that the equation governing v is the same as a passive scalar transport equation. The contours of v, hence, accurately represent the jet on the x–z plane.

In the three–dimensional 'jet in crossflow' problem, the jet has a circular cross–section close to the jet–exit. At least until the jet bends significantly into the crossflow, the behavior of the jet can be imagined to be similar to the behavior of the jet in the model problem. The evolution of the jet in the three–dimensional problem is spatial (moving away from the jet–exit) while the evolution of the jet in the model problem is temporal. The temporal evolution variable (t) can be related to the spatial evolution variable (s) as

$$s = \int_0^t u_s \ \mathrm{dt},$$

where u_s is the local velocity of the jet (in the 3–d problem).

The velocity of the jet is $v_j = u_\infty$, and simulations are performed at Reynolds numbers ($\mathrm{Re} = v_j d/\nu$) of 1000, 10000 and 100000. The mesh used for the simulations has uniform edge lengths $\Delta x/d = 0.005$ and $\Delta z/d = 0.005$. Figure 5 shows the evolution of the center of the jet with time. The center of the jet is defined as the centroid of the vertical velocity (v). Also shown is a quadratic fit to each of the trajectories, denoted by symbols. The initial trajectory of the jet is quadratic while the later trajectory is linear. This suggests that initially, the jet experiences a constant acceleration in the direction of the crossflow, and that it moves at a constant velocity at a later time ($tu_\infty/d > 0.5$, for Re = 1000, from figure 5). The acceleration experienced by the jet may be related to the pressure gradient imposed on it by the crossflow fluid, which suggests that the jet is pressure–driven in the initial stages of evolution and that it is momentum–driven in the later stages. For the jet in crossflow, the implication is that the near–field is pressure–driven whereas the far–field is momentum–driven.

The acceleration experienced by the jet (in the accelerating regime), and the velocity of the jet (in the constant–velocity regime) appear to depend on the Reynolds number. Figure 5 shows that as the Reynolds number increases, the jet experiences a lower initial acceleration. Also, the 'accelerating regime' lasts for a shorter time at higher Reynolds numbers. Increasing the Reynolds number also appears to lower the velocity in the 'constant velocity regime'.

Contours of velocity v at different instants of time in the vicinity of the jet are shown in figure 6. Figures 6(a)–(d) show the solution of the model problem at Re=1000 and figures 6(e)–(h) show the solution at Re=10000. Note that figures in the same row are plotted at the same instant of time. Also, the oscillations observed exterior to the jet are a part of the

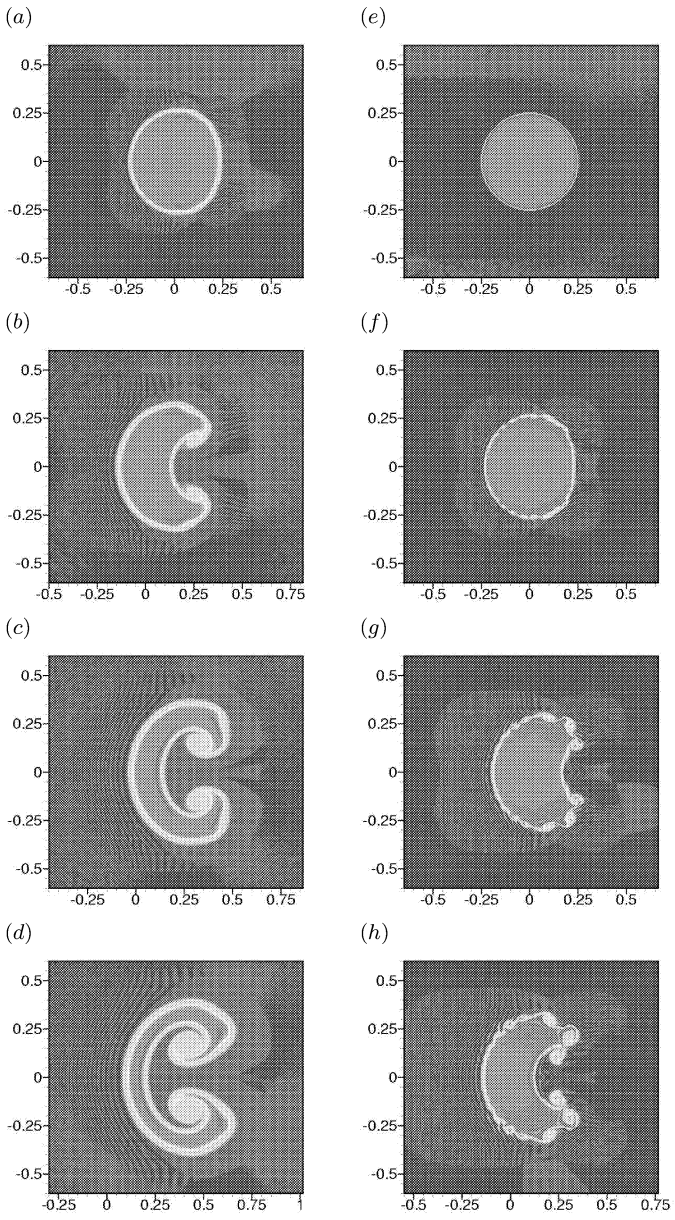

Figure 6: Behavior of the solution of the model problem. (a)–(d) : Re = 1000, (e)–(h) : Re = 10000. Only part of the domain is shown.

solution and not oscillations resulting from the numerics. The oscillations appear to be aligned with the local curvature of the jet, and it was observed that grid refinement does not affect these oscillations.

The jet that is initially circular, begins to flatten at the trailing edge, forming a kidney–shaped cross–section. The trailing edge continues to move towards the leading edge forming a partial 'ring' of jet fluid around crossflow fluid (figure 6(d)). However, the progression rate appears slower at the higher Reynolds number. The deformation the jet experiences can be explained in terms of the pressure field around the jet. The initial pressure field around the jet is symmetric and the maximum pressure is observed at the trailing and leading edges of the jet. The jet also experiences an acceleration in the

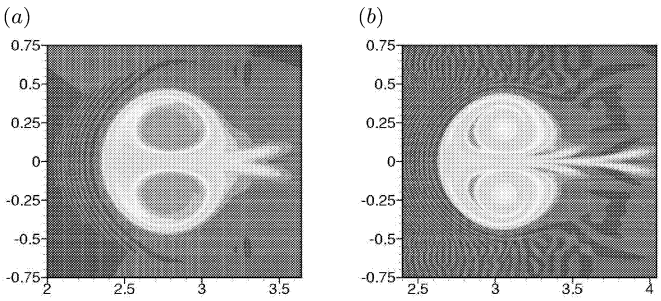

Figure 7: Final stage in the evolution of the jet in the model problem. (a) : Re = 1000, and (b) : Re = 10000. The counter–rotating vortex pair is clearly seen.

streamwise direction. The pressure gradient is in the direction of the acceleration at the leading edge, and in the direction opposing this acceleration at the trailing edge. The symmetry about the z–axis is thus broken, and the jet begins to flatten at the trailing edge. As long as the jet accelerates, the trailing edge continues to move closer to the leading edge.

The Reynolds number has a noticeable effect on the instabilities on the jet edges. At Re =1000, no instabilities are observed. At Re = 10000, however, figures 6(e)-(h) show 'rollers' on the top and bottom edges of the jet. Since the crossflow velocity field is initially that of potential flow past a cylinder, the shear is the greatest at the top and bottom edges of the jet. This results in the Kelvin–Helmholtz instability mechanism being active on these edges. The initial stages of this instability are observed in figure 6(e) and the ensuing 'rollers' are observed in figures 6(f)–(h). According to the initial condition, vorticity (ω_y) is distributed along the jet circumference. As the jet evolves, ω_y accumulates towards the trailing edge of the jet – forming a counter–rotating vortex pair. The CVP is is clearly visible in figures 6(c) & (d). This implies that the pipe is not necessary for the formation of the CVP. The pressure and velocity field in the vicinity of the jet cause the CVP to be formed slightly downstream of it. However, it appears that the contribution to the CVP's vorticity comes from the vorticity in the jet shear layer. With respect to the suggestion by Kelso *et al.* (1996) that there is a connection between the CVP roll–up and the separation inside the pipe, it appears that the separation 'contributes' to the CVP formation rather than 'leads to' it. It must also be mentioned that the separation (and the resulting separation streamlines on the pipe surface) inside the pipe is not evident at higher velocity ratios (Muppidi & Mahesh 2005a : the separation streamlines were observed at $r = 1.52$ and not at $r = 5.7$). The cross–section of the jet in the 'constant velocity regime' is shown in figure 7. The two plots are not at the same instant of time. The jet at Re = 1000 reaches this quasi–steady state earlier than the jet at Re = 10000. Note that even at the higher Re, the instabilities on the jet edge are absent, and CVP is clearly visible. In this regime, the jet moves in the direction of the crossflow at a constant velocity, as shown in figure 5.

SUMMARY

DNS of a round turbulent jet in crossflow at conditions same as the experiments of Su & Mungal (2004) are performed. Velocity and turbulent intensity profiles from the simulation